Full speckle suppression in laser projectors using two Barker code-type optical diffractive elements

Anatoliy Lapchuk[1,], Andriy Kryuchyn[1], Vyacheslav Petrov[1], Victor Yurlov[2] and Volodymyr Klymenko[3]*

[1]*Institute for Information Recording of NAS of Ukraine, Shpak Str. 2, Kiev 03113, Ukraine*

[2]*Samsung Electro-Mechanics Co., Ltd., Suwon 443-743, Korea*

[3]National Aviation University, Cosmonaut Komarov Pr. Kiev 03058, Ukraine

**Corresponding author: alapchuk@yahoo.com*

The mathematical model of a speckle suppression method based on two Barker code-type diffractive optical elements moving in orthogonal directions is developed. The analytic formulae for speckle suppression efficiency are obtained. The model indicates that the one pair of DOE can be used for laser beams of different colors. It is proved that the output numerical aperture of the objective lens equal to $NA = l/T$ provides the maximum speckle suppression effect. The speckle contrast is not dependent on a distance of the viewer to the screen until the distance decreases below the distance where the spatial resolution of the eye on the screen is less than the length of the image of the DOE structure period on the screen. The analysis of the simulated results demonstrates that the method can decrease the speckle contrast to less than 5%, which is below human eye sensitivity, with an optical efficiency greater than 90%.

OCIS codes: 110.6150, 110,1650.

1. Introduction

The use of lasers in projectors and displays provides significant advantages; namely, it allows to obtain high-color saturated images, high optical efficiency and small size. The high optical efficiency and small size are especially important for mobile devices. The engineering advantages and peculiarities of laser projectors are summarized in [1]. However, speckle phenomena arising from the coherence of laser light [2,3] severely degrades the image quality and has inhibited the widespread application of lasers in image systems [1, 4]. The subjective speckle (the speckle created in image systems) are granular light intensity modulation in the image due to the interference effect when coherent light is used for illumination [2,3]. The speckle contrast (C) is used to measure the depth of light intensity modulation caused by speckles. It is defined as the ratio of the standard deviation to the mean of the speckle intensity and is given by the following expression [2, 3]:

$$C = \frac{s_I}{<I>} = \frac{\sqrt{<I^2> - <I>^2}}{<I>} \qquad (1)$$

where s_I, $<I>$ and $<I^2>$ are standard deviation, the mean value and the second moment of light intensity on the screen. Often, it is more convenient to use the speckle suppression coefficient k_{sp} instead of speckle contrast:

$$k_{sp} = 1/C. \qquad (2)$$

Because subjective speckle arise directly in the image system and have a spatial correlation length approximately equal to the spatial resolution of the optical system, it is not practically possible to use special filters for speckle suppression. Therefore, speckle suppression methods are mainly based on speckle pattern averaging. Speckle averaging can be accomplished by using the wavelength, angle or polarization diversity of a laser beam [3]. All of these three factors are

independent and therefore, the speckle suppression coefficient can be represented as the product of three coefficients [3]:

$$k_{sp} = k_{sp}^{l} k_{sp}^{q} k_{sp}^{pol}, \tag{3}$$

where k_{sp}^{l} is the coefficient of speckle contrast suppression due to wavelength diversity, k_{sp}^{q} is that due to angle diversity and k_{sp}^{pol} is that due to polarization diversity ($k_{sp}^{pol} < \sqrt{2}$).

The efficiency of wavelength diversity method can be estimated by the formula [3]:

$$k_{sp}^{l} \sim \left(ph\Delta l / 2\right)^{0.5} / l, \tag{4}$$

where l is laser wavelength, Δl is the laser's spectral bandwidth and h is the average surface-profile height variation of the screen. Theoretical estimation has shown that for full speckle suppression for a screen with a roughness height of approximately 50 μm, the spectral bandwidth should be at least $\Delta l > 50nm$. The time coherence of the laser beam can be reduced by using several lasers [5-7] or by using a broadband laser [8]. For speckle averaging using several lasers with equal light intensity and with wavelength differences sufficient to create different speckle patterns (the best case for speckle suppression), the speckle contrast can be decreased at most to a level of [2]

$$C = \frac{C_0}{\sqrt{N}}, \tag{5}$$

where C is the final speckle contrast, C_0 is the speckle contrast in the case of using one laser (~0.6), and N is the number of lasers. It is clear from Eq. (5) that over 100 lasers, with a total spectral bandwidth approximately equal to 10%, are required to suppress speckle noise below the sensitivity of the human eye. However, using many lasers for illumination is usually unacceptable due to the complexity and significant increase of the size of the projector. The application

of a broadband laser for illumination results in low optical efficiency and small speckle suppression due to the low efficiency and small spectral bandwidth of broadband lasers [9].

The most effective speckle suppression can be obtained by using angle diversity. The angle diversity can be obtained in several ways: 1) by the vibration of a screen, 2) by vibrating diffractive optical elements (DOE) inside the optical system, 3) by beam scanning along the illumination surface, and 4) by de-correlation of the illumination beams incident from different angles simultaneously.

The rapid movement or vibration of a screen [10] is not an optimal and acceptable solution for almost all technical applications.

It is possible to achieve large speckle suppression by moving or vibrating a random diffuser inside optical systems [11-13]. Full speckle suppression can be obtained by a rapidly vibrating diffuser [13]. However, the use of a random diffuser requires high-frequency and large-amplitude of DOE vibration, and the method has high optical losses.

The original method of speckle suppression was proposed by Trisnadi [14, 15]. Trisnadi proposed using a periodic DOE with a specially structure instead of a random diffuser. More specifically, Trisnadi proposed the use of a DOE with phase modulation of the laser beam wavefront based on the Hadamard matrix algorithm. It was proved that method allows obtaining high optical efficiency and high level of speckle suppression. However, the method requires very accurate, fast and complex DOE movement, which is very difficult to realize in technical devices. A prior study [16] reports on a modification of the Trisnadi method in which the 2D structure of the DOE is changed to a pair of 1D DOE structures that together realized the Hadamard matrix modulation method. The improvement can be useful for speckle suppression only in the case of being able to switch a DOE structure by voltage, for example, by using a

DOE based on liquid crystal meshes. However, for efficient speckle suppression, the frequency of switching of liquid crystal panel meshes should be greater than 15000 Hz, which is far above the maximum switching frequency of modern liquid crystal elements (approximately 1000 Hz).

It is possible to obtain high speckle suppression by laser beam scanning along the screen by a vibrating mirror in the Fourier plane of the objective lens. The value of the numerical aperture of the objective lens is the parameter that determines the effect of speckle suppression in this method [3, 17]. The method can be used in 1D laser projectors [18-20] and in laser pointer projectors [21-22]. However, because a laser pointer projector cannot use a large mirror due to the requirement of very rapid mirror vibration, the method is effective only for 1D scanning laser projectors. A simple and effective (with small optical losses) method of homogeneous filling of the aperture of the objective lens by laser illumination is proposed in [17, 23]. The Barker code-type DOE is used to generate a wide spatial frequency band and to increase the beam width to a diameter of the input numerical aperture of objective lens independent of the initial width of the laser beam. In [24,25], a generalization of this method was proposed. However in the method, only an aperture along the beam scanning direction can be used for speckle suppression. Significant optical system complication is required for the use of an aperture in the orthogonal direction for speckle suppression [26]. A speckle contrast in the range of 14-18% was obtained using this method [23].

In recent years, several novel methods of speckle suppression have been developed based on a light pipe tube [27, 28]. The effect of speckle suppression (using the angle diversity of the illumination system) in this method is obtained by vibration or rotation of the pipe tube. The method requires the movement of a large diameter (several centimeters) and long (at least several diameters) light pipe tube.

Several groups have reported on the use of a multimode fiber to reduce speckle contrast in laser projectors [29–32]. The theory behind this method was developed by Goodman [33]. The length of fiber should be long enough to achieve de-correlation of practically all fiber modes. It is possible to achieve a speckle contrast of 0.01 at the distant end of the fiber ends when the fiber is several meters long [33]. The greatest advantage of this method is that it does not require mechanical movement. However, the correlation length of incident laser beam on screen increases by a factor equal to the magnification of the optical system [34]. Therefore, to preserve the same speckle contrast on the screen as that at the distant fiber end, the method requires the number of multimode fibers be approximately equal to the square of the magnification of the projector objective lens (approximately equal to the number of pixels on the screen > 300000).

Despite significant efforts to develop a simple method and a compact system for decreasing speckle noise to an acceptable for the human eye level, this problem has not been solved until now. Below, we describe the theory of an efficient and simple speckle suppression method based on two moving Barker code DOEs, which decreases speckle contrast below human eye sensitivity (with optical losses less than 10%).

2. Optical scheme

The optical scheme of a laser projector with a new speckle suppression mechanism is shown in Fig. 1. In the speckle suppression part, a laser beam passes through two diffractive optical elements situated close to each other (distance between them is significantly smaller than the objective lens focal length). The DOE should be placed in the illumination part or in the object plane or in the plane of the intermediate image plane of the optical system. Each DOE structure is a 1D Barker code-type DOE, as shown in Fig. 2. The Barker code is a sequence of N numbers of B_i taking values of 1 or -1, which produces the narrowest autocorrelation peaks [35]. The

Barker code-type DOE is a 1D periodic two level structure (see Fig. 2), where the difference in height provides a phase shift on half of wavelength; as a result, the transmitted electromagnetic field at the back surface of the DOE is modulated by a periodic Barker code sequence. The DOE period on the screen (in the image plane) is equal to $T_0 = NT$, where T is the DOE pitch length, N is the Barker-code length and D is the width of the main maximum of the point-spread function of the human eye on a screen. One DOE structure is stretched along the x axis, and it diffracts light along the X direction. Another DOE has its structure stretched along the y axis, and it diffracts light along Y direction. Each of these structures is moving in the image plane along its diffraction plane. The objective lens projects light onto a screen. The optical modulator modulates the intensity of the light to create an image on the screen. However, because we are only interested in investigating the electric-field modulation caused by speckle, it is assumed that the screen is homogeneously illuminated.

The complete optical system (projector and viewer) has three numerical apertures. The first aperture is the input numerical aperture, $NA_1 = \sin q_1$, of the objective lens of the projector. The input numerical aperture serves as a low-pass filter of spatial frequency and therefore distorts the image and decreases the optical efficiency. The second is the output numerical aperture, $NA = \sin q$, of the objective lens which determines the maximum possible resolution of the projected image on the screen. The third aperture is the input numerical aperture, $NA_3 = \sin q_3$, of the eye, which determines the resolution of the eye on the screen.

The optical system of the projector is assumed to have no aberrations. In spite of an aberration-free optical system, the phase modulation of the light on the screen will be disturbed due to spatial frequency truncation by a numerical aperture of objective lens, $NA_1 < 1$. The actual pitch of the DOE has a width of T_1. A ratio $k_p = NA_1 / (l / T_1)$ determines the accuracy of the

phase reproduction on the screen. Because $T/T_1 = NA_1/NA$, we can rewrite the ratio as $k_p = NA/l/T$, and the last ratio determination will be used to characterize the optical system limitation on the spatial frequency band. The ratio of the one period of the DOE structure at image on screen $T_0 = NT$ to the eye (photo camera) resolution on the screen (by Rayleigh), $D_0 = D/2 = l/2NA_3$, is another important parameter that determines the speckle suppression efficiency and will be used below in the analysis of the method.

3. Mathematical model

First, we assumed that we have an ideal optical system (aberration free) with a large input numerical aperture, $k_p = NA_1/l/T_1 >> 1$; therefore, we can exactly reproduce the Barker code wavefront phase modulation onto a screen (with a magnification). Below, we also assumed that the Barker code length N and period of both DOEs (vertical and horizontal) are equal to each other; however, the obtained results can be easily generalized for cases with different Barker code lengths and periods.

When using one moving Barker code-type DOE, we will obtain approximately the same effect as that obtained in a 1D laser projector with a Barker code DOE [17, 24].We also assumed that the aperture of the objective lens of a viewer (human eye or photo camera) is square (instead of circular) to simplify the analyses of the 2D case. Changing the shape of the aperture from circular to square should not significantly influence speckle suppression; however, it permits a simple analytical expression for the speckle suppression efficiency. It is easy to generalize the algorithm for a circular aperture by changing the point-spread function of the objective lens; however, in this case, a large amount of calculations are required to determine the speckle parameters.

All the results are obtained in the Fresnel scalar approximation using the thin-lens model for the objective lens. Because the output numerical aperture used in the projection system is small (NA<<1), the Fresnel scalar approximation is accurate.

The electric-field distribution at the screen can be written as follows:

$$E_{scr}(x,y) = E_0(x,y)H(x-V_1t)H(y-V_2t), \tag{6}$$

where $E_0(x,y)$ is the electric-field amplitude distribution at the screen for the optical scheme without a DOE, $H(x)$ is one DOE modulation function scaled due to the magnification of the objective lens of the projector, and V_1, V_2 are the DOE image scanning velocities on the screen. In the Fresnel approximation [36, 23], the complex amplitude of the field on the retina of a viewer can be written as follows:

$$E(x,h,t) = \frac{\Delta E_0}{l\sqrt{a^2b^2}} \cdot \int_{-\infty}^{\infty} r(x,y)H(x+V_1t)H(y+V_1t)\exp\left(-ik\left(x^2+y^2\right)/2a\right)\sin c\left\{\frac{2p}{D}\left(\frac{a}{b}x+x\right)\right\}\sin c\left\{\frac{2p}{D}\left(\frac{a}{b}h+y\right)\right\}dxdy \tag{7}$$

where x and y and x and h are the coordinates at the screen and the retina, respectively, t is the time, Δt is one time resolution of the human eye, Δ is the crystalline lens diameter, l is the wavelength, $k = 2p/l$ is the wavenumber, $\sin c(x) = \sin(x)/x$, and $r(x,y)$ is the random screen complex field amplitude reflection coefficient defined by the screen micro-roughness. Below, we will ignore the phase factor $\exp\left(-ik\left(x^2+y^2\right)/2a\right)$ in Eq. (7) because any photo-sensor (as well as the human retina nerves) is sensitive only to the optical intensity.

It is assumed that the first DOE structure is shifted by one of its period during one resolution time of the eye, Δt_0 (along the x axis). The second DOE velocity, V_2, is assumed to be larger than V_1 by a factor of MN, where M is a nonzero integer number. Hence, the second

DOE is shifted by the length of *MN* periods of DOE structure during time interval of Δt_0 Δt_0(along the y axis). The image recreated in the human eye can be calcula ted as the squared modulus of the field amplitude (Eq. (7)) integrated over the time interval Δt_0:

$$\begin{aligned} I(x,y) &= \frac{1}{\Delta t_0}\int_{\Delta t_0}\left|E(x,y)\right|^2 dt = \\ &= G_0 E_0^2 \int_{-\infty}^{\infty}\int_{-\infty}^{\infty}\int_{-\infty}^{\infty}\int_{0}^{N\Delta t_0} r(x_1,y_1)r^*(x_2,y_2)Sinc\left[\frac{2p}{D}(x+x_1)\right]Sinc\left[\frac{2p}{D}(x+x_2)\right]Sinc\left[\frac{2p}{D}(y+y_1)\right] \\ &\quad Sinc\left[\frac{2p}{D}(y+y_2)\right]e^{-jk\frac{x_1^2-x_2^2+y_1^2-y_2^2}{2a}}Ad(x_1,x_2,y_1y_2)dx_1dx_2dy_1dy_2 \end{aligned} \tag{8}$$

where *I(x,y)* is the human eye image related to the screen coordinates $x = \frac{a}{b}x$ and $G_0 = \frac{\Delta^2}{l^2a^2b^2}$;

$$\begin{aligned} Ad(x_1,x_2,y_1,y_2) &= \frac{1}{TV_1}\int_T H(x_1-V_1t)H^*(x_2-V_1t)H(y_1-V_2t)H^*(y_2-V_2t)dt = \\ &= \frac{1}{TV_1}\int_{-NT/2}^{NT/2} H(x)H^*(x+x_2-x_1)H\left(xN*mv+y_1-\frac{v_2}{v_1}x_1\right)H^*\left(xN*Mv+y_2-\frac{v_2}{v_1}x_1\right)dx \end{aligned} \tag{9}$$

The screen has a rough surface with a roughness height considerably greater than the wavelength of the light. Therefore, we can write $\langle r(x_1,y_1)r^*(x_2,y_2)\rangle = Rd(x_1-x_2)d(y_1-y_2)$, where the brackets $\langle\ \rangle$ denote screen averaging and R is the mean intensity reflection coefficient. Then, the expression for the mean value of the light intensity can be written as follows:

$$\begin{aligned} \langle I(x,y)\rangle &= G_0E_0^2R\iint\iint Sinc^2\left[\frac{2p}{D}(x+x_1)\right]Sinc^2\left[\frac{2p}{D}(y+y_1)\right]Ad(x_1,x_1,y_1,y_1)dx_1dy_1 = \\ &= G_0E_0^2R\iint\iint Sinc^2\left[\frac{2p}{D}x_1\right]Sinc^2\left[\frac{2p}{D}y_1\right]A(x_1,x_1,y_1,y_1)dx_1dy_1 \end{aligned} \tag{10}$$

The mean of the square of the light intensity can be written as follows:

$$\langle I^2\rangle = = E_0^4 G0^2 \iiint\!\!\iint F(x_1,x_2,x_3,x_4,y_1,y_2,y_3,y_4) A(x_1,x_2,y_1,y_2) Sinc\left[\frac{2p}{\mathrm{D}}x_1\right] Sinc\left[\frac{2p}{\mathrm{D}}x_2\right] Sinc\left[\frac{2p}{\mathrm{D}}y_1\right] Sinc\left[\frac{2p}{\mathrm{D}}y_2\right] \times$$
$$\times A(x_3,x_4,y_3,y_4) Sinc\left[\frac{2p}{\mathrm{D}}x_3\right] Sinc\left[\frac{2p}{\mathrm{D}}x_4\right] Sinc\left[\frac{2p}{\mathrm{D}}y_3\right] Sinc\left[\frac{2p}{\mathrm{D}}y_4\right] e^{-jk\frac{x_1^2-x_2^2+x_3^2-x_4^2}{2a}} e^{-jk\frac{y_1^2-y_2^2+y_3^2-y_4^2}{2a}} dx_1dx_2dx_3dx_4dy_1dy_2dy_3dy_4 \quad (11)$$

where
$$F(x_1,x_2,x_3,x_4,y_1,y_2,y_3,y_4) = \langle r(x_1,y_1) r^*(x_2,y_2) r(x_3,y_3) r^*(x_4,y_4)\rangle =$$
$$= R^2 \begin{bmatrix} d(x_1-x_2)d(x_3-x_4)(y_1-y_2)d(y_3-y_4) + \\ +d(x_2-x_3)d(x_1-x_4)d(y_2-y_3)d(y_1-y_4) \end{bmatrix} \quad (12)$$

Using Eq. (12), we can rewrite Eq. (11) as follows:

$$\langle I^2\rangle = In_1 + In_2, \quad (13)$$

where

$$In_1 = R^2 E_0^4 G_0{}^2 \iiint\!\!\iint d(x_1-x_2)d(x_3-x_4) Ad(x_1,x_2,y_1y_2) Ad(x_3,x_4y_3,y_4) Sinc\left[\frac{2p}{\mathrm{D}}x_1\right] Sinc\left[\frac{2p}{\mathrm{D}}x_2\right] \times$$
$$\times Sinc\left[\frac{2p}{\mathrm{D}}x_3\right] Sinc\left[\frac{2p}{\mathrm{D}}x_4\right] e^{-jk\frac{x_1^2-x_2^2+x_3^2-x_4^2}{2a}} Sinc\left[\frac{2p}{\mathrm{D}}y_1\right] Sinc\left[\frac{2p}{\mathrm{D}}y_2\right] Sinc\left[\frac{2p}{\mathrm{D}}y_3\right] Sinc\left[\frac{2p}{\mathrm{D}}y_4\right] e^{-jk\frac{y_1^2-y_2^2+y_3^2-y_4^2}{2a}}$$
$$d(x_1-x_2)d(x_3-x_4)dx_1dx_2dx_3dx_4dy_1dy_2dy_3dy_4 = \quad ,(14a)$$
$$= R^2 E_0^4 G_0{}^2 \iint Ad(x_1,x_1,y_1y_1) Sinc^2\left[\frac{2p}{\mathrm{D}}x_1\right]\left[\frac{2p}{\mathrm{D}}y_1\right] dx_1dy_1$$
$$\iint Ad(x_3,x_3y_3,y_3) Sinc^2\left[\frac{2p}{\mathrm{D}}x_3\right] Sinc^2 Sinc^3\left[\frac{2p}{\mathrm{D}}y_3\right] dx_3dy_3 = \langle I\rangle^2$$

$$In_2 = R^2 E_0^4 G_0{}^2 \iiint\!\!\iint Ad(x_1,x_2,y_1,y_2) Ad(x_3,x_4,y_3,y_4) Sinc\left[\frac{2p}{\mathrm{D}}x_1\right] Sinc\left[\frac{2p}{\mathrm{D}}x_2\right] Sinc\left[\frac{2p}{\mathrm{D}}y_1\right] Sinc\left[\frac{2p}{\mathrm{D}}y_2\right] \times$$
$$\times Sinc\left[\frac{2p}{\mathrm{D}}x_3\right] Sinc\left[\frac{2p}{\mathrm{D}}x_4\right] Sinc\left[\frac{2p}{\mathrm{D}}y_3\right] Sinc\left[\frac{2p}{\mathrm{D}}y_4\right] e^{-jk\frac{x_1^2-x_2^2+x_3^2-x_4^2}{2a}} e^{-jk\frac{y_1^2-y_2^2+y_3^2-y_4^2}{2a}} \quad (14b)$$
$$d(y_2-y_3)d(y_1-y_4)d(x_2-x_3)d(x_1-x_4)dx_1dx_2dx_3dx_4dy_1dy_2dy_3dx_4 =$$
$$= R^2 E_0^4 G_0{}^2 \iiint\!\!\iint |Ad(x_1,x_2y_1,y_2)|^2 Sinc^2\left[\frac{2p}{\mathrm{D}}x_1\right] Sinc^2\left[\frac{2p}{\mathrm{D}}x_2\right] Sinc^2\left[\frac{2p}{\mathrm{D}}y_1\right] Sinc^2\left[\frac{2p}{\mathrm{D}}y_2\right] dx_1dx_2dy_1dy_2$$

Substitution of Eq.(13, 14) into Eq. (1) yields the following formula for speckle contrast:

$$C = \sqrt{\frac{\iint\!\!\iint |Ad(x_1,x_2,y_1,y_2)|^2 Sinc^2\left[\frac{2p}{\mathrm{D}}x_1\right] Sinc^2\left[\frac{2p}{\mathrm{D}}y_1\right] Sinc^2\left[\frac{2p}{\mathrm{D}}x_2\right] Sinc^2\left[\frac{2p}{\mathrm{D}}y_2\right] dx_1dx_2dy_2dy_2}{\left(\iint Sinc^2\left[\frac{2p}{D}(x_1)\right] Sinc^2\left[\frac{2p}{D}(y_1)\right] A(x_1,x_1,y_1,y_1) dx_1dy_1\right)^2}} \quad (15)$$

Because the two DOEs are periodic structures, the autocorrelation function (9) can be written as a sum of N integrals as follows:

$$Ad(x_1, x_2, y_1, y_2) = \frac{1}{\Delta t_0 V_1} \int_0^{\Delta t_0} H(xNM + y_1 - N*mx_1) H^*(xN*M + y_2 - N*mx_1) \sum_{k=0}^{N-1} H(x + k*T) H^*(x + k*T + x_2 - x_1) dx \tag{16}$$

It is easy to show that the sum in Eq. (16) does not depend on x and therefore can be written as follows:

$$A_0(x_2 - x_1) = \sum_{k=0}^{N-1} H(x + k*T) H^*(x + k*T + x_2 - x_1) = \sum_{n=1}^{N} B_i B_{i+k} \tag{17}$$

where $A_0(x_2 - x_1)$ is the discrete autocorrelation function of the periodic Barker code sequence (autocorrelation function of the discrete Barker code sequence). Using Eq. (17), we can rewrite formula (16) as

$$A(x_1, x_2, y_1, y_2) = \frac{A_0(x_2 - x_1)}{N*Mv*TV_1} \int_0^{NMvT} H(x* N*Mv + y_1 - N*mx_1) H^*(x* N*Mv + y_2 - N*mx_1) dN*Mvx = \\ = \frac{A_0(x_2 - x_1)}{N*TV_1} \int_0^{NT} H(u + y_1) H^*(u + y_2) du = CA_0(x_2 - x_1) A(y_2 - y_1) \tag{18}$$

where $A(x_2 - x_1) = \int_0^{NT} H(u + x_1) H^*(u + x_2) du$ is the autocorrelation function of the periodic Barker code function. By substituting Eq. (18) into Eq. (15), the formula for speckle contrast can be rewritten as follows:

$$C = \frac{\sqrt{\iint |A_0(x_2 - x_1)|^2 Sinc^2\left[\frac{2p}{D} x_1\right] Sinc^2\left[\frac{2p}{D} x_2\right] dx_1 dx_2 \iint |A(y_2 - y_1)|^2 Sinc^2\left[\frac{2p}{D} y_1\right] Sinc^2\left[\frac{2p}{D} y_2\right] dy_1 dy_2}}{A_0(0) A(0) \iint Sinc^2\left[\frac{2p}{D}(x_1)\right] Sinc^2\left[\frac{2p}{D}(y_1)\right] dx_1 dy_1} \tag{19}$$

By changing the variable $u_1 = x_1$, $u_2 = x_2 - x_1$, $v_1 = y_1$, $v_2 = y_2 - y_1$, Eq. (16) can be rewritten

as follows:

$$C=\frac{\sqrt{\iint\left|A_0(u_2)\right|^2 Sinc^2\left[\frac{2p}{\mathrm{D}}u_1\right]Sinc^2\left[\frac{2p}{\mathrm{D}}(u_1+u_2)\right]du_1du_2\int\int\left|A(v_2)\right|^2 Sinc^2\left[\frac{2p}{\mathrm{D}}v_1\right]Sinc^2\left[\frac{2p}{\mathrm{D}}(u_1+u_2)\right]dv_1dv_2}}{A_0(0)A(0)\iint Sinc^2\left[\frac{2p}{D}(x_1)\right]Sinc^2\left[\frac{2p}{D}(y_1)\right]dx_1dy_1} \quad (20)$$

and finally, we obtain:

$$C=C_x*C_y=\frac{1}{\sqrt{2}}2\sqrt{\int_{-\infty}^{\infty}\left|\frac{A_0(Du)}{A_0(0)}\right|^2 Q(u)du}\,2\sqrt{\int_{-\infty}^{\infty}\left|\frac{A(Dv)}{A(0)}\right|^2 Q(v)dv} \quad (21)$$

where [23] $Q(u)=\int_{-\infty}^{\infty}\sin c^2[2p(u+x)]\sin c^2[2px]dx=\frac{1-\sin c^2(4pu)}{8p^2u^2}$,

$$C_x=2\sqrt{\int_{-\infty}^{\infty}\left|\frac{A_0(Du)}{A_0(0)}\right|^2 Q(u)du}\,, \quad (22a)$$

$$C_y=2\sqrt{\int_{-\infty}^{\infty}\left|\frac{A(Dv)}{A(0)}\right|^2 Q(v)dv} \quad (22b)$$

In Eq. (21) a factor $1/\sqrt{2}$ is added to take into account depolarization properties of the screen.

4. Simulation results in the approximation of an ideal optical system and an ideal Barker code-type DOE

The graph of the normalized autocorrelation functions $A(x)/A(0)$ and $A_0(x)/A_0(0)$ (not scaled) and function $Q(x)$ are shown in Fig. 3. Both $A(x)$ and $A_0(x)$ autocorrelation functions have periodic high and narrow (width of T) peaks that have triangle and rectangular shapes, respectively. The normalized autocorrelation functions have peak values of 1, and outside the peaks areas, these functions have an absolute value equal to or smaller than 1/N. For a large *N*, the *Q* function is nearly constant inside the narrow peaks of the autocorrelation functions, and it

is possible to simplify the formulae for speckle contrast. Formula for $C_x^{\,2}$ can be written as:

$$C_x^{\,2} = 4\frac{\int_{-\infty}^{\infty}\left|A_0(Du)\right|^2 Q(u)du}{A_0(0)} \approx 4\sum_{i=-\infty}^{\infty} Q(iNT/D)\int_{-T/2D}^{T/2D} dx + s_1 = \frac{4T}{D}\sum_{i=-\infty}^{\infty} Q(iNT/D) + s_1 \quad (23a)$$

where $s_1 < 4\int_{T/2D}^{\infty}\frac{\left|A(Dv)\right|^2}{\left|A(0)\right|^2}Q(v)dv < \frac{4}{N^2}\int_{-\infty}^{\infty}Q(v)dv = \frac{1}{N^2}$,

and for $C_y^{\,2}$:

$$C_y^{\,2} = 2\int_{-\infty}^{\infty}\frac{\left|A(Dv)\right|^2}{\left|A(0)\right|^2}Q(v)dv \approx 2\sum_{i=-\infty}^{\infty} Q(iNT/D)\int_{-T/D}^{T/D}(1-xD/T)^2\,dx + s_2 = \frac{4T}{3D}\sum_{i=-\infty}^{\infty} Q(iNT/D) + s_2, \quad (23b)$$

where $s_2 < 4\int_{T/D}^{\infty}\frac{\left|A_0(Dv)\right|^2}{\left|A(0)\right|^2}Q(v)dv < \frac{4}{N^2}\int_{-\infty}^{\infty}Q(v)dv = \frac{1}{N^2}$.

For a large *N*, it is possible to reject terms s_1 and s_2 in Eq. (23) (with a minor loss in accuracy in the calculation of order $\frac{1}{N^2}$):

$$C_x^{\,2} \approx \frac{4T}{D}\sum_{i=-\infty}^{\infty} Q(iNT/D) \quad (24)$$

$$C_y^{\,2} \approx \frac{4T}{3D}\sum_{i=-\infty}^{\infty} Q(iNT/D) \quad (25)$$

The half width of the *Q* function is approximately equal to 0.5 (see Fig.4). Therefore, when one period of the DOE is larger than $D/2=D_0$, only one maximum of the correlation function is inside a central peak of the *Q* function, and with good accuracy, only one term with an index i=0 can be left in the sums (24, 25) for the calculation of $C_x^{\,2}$ and $C_y^{\,2}$:

$$C_x^{\,2} \approx \frac{4T}{D}Q(0) = \frac{2}{3N_0} \quad (26)$$

$$C_y^{\,2} = \frac{8T}{3D} Q(0) = \frac{4}{9N_0} \tag{27}$$

where $N_0 = D_0 / T$ is the number of DOE pitches inside one eye resolution.

Fig. 5 shows the simulation results of the speckle contrast calculated using three different approximations. The analysis of the numerical results obtained by the exact formula (20) has shown that for a large D_0 ($D_0/NT>1$), the speckle contrast is independent of D_0 and it is close to $C = 1/\left(N\sqrt{3}\right)$. As D_0 decreases to values below the DOE structure period on screen, the speckle contrast rapidly increases and approaches the level of an optical system without a DOE $C = 1/\sqrt{2}$ when the DOE pitch width T exceeds D. Because the resolution of the eye at the screen is proportional to the distance to the screen, Fig. 5 also exhibits a dependence of speckle suppression on the distance to the screen (upper axis on Fig. 5) of viewer. The speckle contrast is nearly independent on S until it decreases below the distance S_0 at which $D_0=NT$. Because of the rapid increase in the speckle level when the distance to the screen is lower than S_0, this area should be avoided by viewers.

The comparison of the numerical results of the speckle contrast obtained by accurate calculation (Eq. 21) and by narrow peak approximation (Eq. (23, 25)) indicate (see Fig. 5) that the latter approximation is quite accurate, with an error of several percent, which is an error level that is sufficient for engineering applications. Therefore, the simplified Eq. (24, 25) can be successfully used in engineering calculations. The simple approximation that takes into account only one of the autocorrelation peaks (see Fig. 6), given by Eq. (26, 27), is correct only for small D ($D<T_0$) when only one of the peaks of the autocorrelation function is inside the central $Q(x)$ maximum.

5. Simulation of the optical system with an arbitrary numerical aperture and a Barker code DOE without an exact phase shift

In an actual optical system, an objective lens has a finite numerical aperture, which truncates high spatial frequencies and therefore cause image blurring. In addition, because the same pair of DOEs is used for laser beams of different colors in our optical scheme (see Fig. 1), the phase shift of the wavefront of some of these beams after transmission through the DOE would not be exactly equal to π (for red and blue beams, for example). However, all of the numerical results described above were obtained under the assumption of an exact phase shift of p by the DOE and of an ideal optical system. In this assumption, we demonstrated that the autocorrelation function of the illuminated laser beam can be represented as a product of two factors (Eq. 21). Independence of the sum in Eq. (16) on the variable x is a basis for the representation of the speckle contrast as a product of two factors, $C_x * C_y$. It is clear that the independence of the autocorrelation function A_0 on x will also be valid in the case of any phase shift (any sequence of two complex numbers but not just in a sequence of 1 and -1) for the ideal optical system; therefore, it will be valid for any color of beam (the proof will be published elsewhere). It is not difficult to show that autocorrelation function A_0 of the optical system with a finite numerical aperture NA_1, due to the linearity and uniformity of the optical transfer function will not depend on x (the proof will be published elsewhere). Therefore, the sum in Eq. (16) would also not depend on x for the case of objective lens with finite numerical aperture and for DOEs without an exact π phase shift. Therefore, it is still correct to use Eq. (20- 22) for the speckle contrast calculation. However, $A_0(x)$ and $A(x)$ in these formulae should be calculated by taking into account the real phase shift and image blurring due to the truncation of high spatial frequencies.

Because speckle contrast is a product of two factors related to two different DOEs moving in two orthogonal directions, we analyzed each factor separately. Sometimes it is more convenient in the analysis of the method to use speckle suppression coefficients instead of speckle contrast, which are determined as follows:

$$k_{sp} = 1/C; \quad k_{sp}^{x} = 1/C_x; \quad k_{sp}^{y} = 1/C_y. \tag{28}$$

Because nearly all projectors have large magnification, the distance from objective lens of projector to the screen is significantly longer than a focal length and the object plane is close to the focal plane. Therefore, the objective lens is represented in the mathematical model as a low-pass filter of spatial frequency with a cutoff frequency of $k_{cutoff} = \frac{2p}{l} NA_1$. The field on the screen is calculated using a direct and inverse Fourier transform (with truncated high spatial frequencies for image calculation) with image rescaling in accordance to the system magnification. The autocorrelation functions $A_0(x)$ and $A(x)$ are calculated using direct numerical integration. All of the calculations below were performed for the optimal ratio of D to T_0 equal to $D/T_0 = 2$ and for a depth of the DOE relief that provides a phase shift of the wavefront of p for a wavelength $l_{gr} = 0.532\,mm$. Because the diffraction angle has a linear dependence on λ and the effect of speckle suppression is based on diffraction phenomena, the optical system will truncate different high spatial frequency ranges for laser beams with different wavelengths, and that difference is taken into account in our mathematical model.

Fig. 6 shows the dependence of the speckle suppression coefficient k_{sp}^{y} on the laser beam wavelength for different output numerical apertures NA of the objective lens. For a small numerical aperture, the objective lens truncates all spatial frequencies of the diffracted beam, with the exception of a small area near zero. Therefore the beam at screen has flat wavefront and

the speckle contrast is close to the speckle contrast of a screen homogeneously illuminated by a plane wave (equal to 1) and does not change with the wavelength. For a large NA, e.g., NA/(λ_{gr}/T) = 3, the maximum speckle suppression is at $l = 0{,}532\,mm$, where the wavefront along the *y* axis on screen corresponds to a periodic Barker code sequence and the amplitude of electromagnetic field has a narrow autocorrelation function. Speckle suppression is significantly smaller for red and blue beams where waterfront of beam has different from Barker code shape. Fig. 7 shows the autocorrelation function of the field on the screen when using a Barker code-type DOE of length N=13. Beams of different colors exhibit autocorrelation peaks of the same width. However, the level of the autocorrelation function outside of the peaks increases when wavelength shifts from the optimal value (the value which provides a wavefront shift of π). It can be shown that for a large numerical aperture (NA/(λ_{gr}/T)>>1), the shift in the wavelength from optimal value of $l = 0{,}532mm$ does not change the width of the normalized autocorrelation function $A_f / A(0)$ but increases the level of the plateau outside the peaks, which can be calculated as follows:

$$A_f / A(0) = A_{f0} / A(0) + \left(1 - A_{f0} / A(0)\right)\sin^2\left(\frac{p\, l_{gr}}{2\, l}\right) \qquad (29)$$

The decrease of the modulation depth of the autocorrelation function *A(x)* (increased plateau level) with a shift of the wavelength from the optimal value results in a speckle suppression coefficient decrease (see Fig. 6).

Fig. 8 shows the dependence of the speckle suppression coefficient k_{sp}^{y} on the numerical aperture for red, green and blue laser beams. The same pair of DOEs that provide a shift in the wavefront of π for a green beam are used for all the laser beams. The speckle suppression coefficient k_{sp}^{y} monotonously increases with an increase of the numerical aperture and has

plateaus for the large numerical apertures ($NA/l/T>1$) for all three beams. A value of the numerical aperture greater than $NA=l_{gr}/T$ is excessive for an optical system because nearly all the light is diffracted inside that angle (see Fig. 9), and a further increase has no significant influence on the speckle suppression. A decrease in the numerical aperture of the objective lens results in an increase in the width and a smoothing of the shape of the peaks of the autocorrelation function (see Fig. 10). The increase in the width of peaks of the autocorrelation function leads to a decrease in the speckle suppression.

The speckle suppression coefficient k_{sp}^{x} exhibits a more complex dependence on the numerical aperture of objective lens (see Fig.11). The speckle suppression coefficient k_{sp}^{x} initially rapidly increases and reaches the first high maximum at $NA/l/T=1$. Subsequently, the value of the coefficient oscillates with decreasing amplitude, and all peaks are lower than first peak. Fig. 12 shows the autocorrelation function of $A_0(x)$ for numerical apertures corresponding to the first and second maxima of the speckle suppression coefficient k_{sp}^{x}. The two autocorrelation functions have the same peak widths and the same levels in the area outside of the peaks. The autocorrelation function in second maximum is closer to the autocorrelation function of the ideal optical system shown in Fig. 3 c. The autocorrelation function $A_0(x)$ in the first maximum of the speckle suppression coefficient has significantly higher peaks (higher depth of modulation) that lead to an increase of the speckle suppression coefficient. The autocorrelation function $A_0(x)$ changes with the shift from the optimal wavelength in a manner similar to the function $A(x)$. With a shift of wavelength from the optimal value (green laser wavelength with a phase shift of π), the width of the peaks is preserved and the level of the plateau around the peaks increases (Fig. 13), thereby decreasing the speckle suppression coefficient. From the numerical results presented in Fig. 11, it follows that there is an optimal

numerical aperture for the speckle suppression coefficient. An increase or decrease in the numerical aperture from the optimal value leads to a decrease in the speckle suppression coefficient k_{sp}^{x}.

6. Conclusion

The method and mathematical model of the speckle suppression mechanism based on two Barker code-type DOEs enables a speckle-free image to be produced by laser projectors. The simple formulae for the speckle contrast calculation were determined. Speckle suppression was determined to be represented as a product of two factors, each of which depends on its own DOE parameters. High speckle suppression can be obtained using the same pair of DOEs for laser beams of different color. The optimal numerical aperture of the objective lens is equal to $NA = l / T$, which provides the maximum speckle suppression.

The analysis demonstrated that the method permits to decrease the speckle contrast below the human eye sensitivity with an optical efficiency larger than 90%. The speckle contrast in the method is not dependent on the distance of the viewer to the screen until the distance decreases below the distance where the resolution of the eye on the screen is less than the DOE structure image on the screen.

A square aperture was used to simulate the eye in the mathematical model to simplify the obtained formulae. The model can be easily generalized to the actual case of a circular aperture for the eye. Additional analysis is required for accurate method optimization to take into account the actual shape of the aperture (circular shape).

6. References

1. Chellappan K. V., Erden E., Urey H. "Laser-based displays: a review," Appl. Opt., **49**(25), F79-F98, (2010).

2. J.C. Dainty, *Laser speckle and related phenomena*. (Spinger-Verlag, 1975).

3. J.W. Goodman, *Speckle Phenomena in Optics. Theory and applications*. (Roberts&Company, 2006).

4. Janssens P., Malfait K., "Future prospects of high-end laser projectors," Proc. SPIE **7232**, 7232-34, (2009).

5. George N., and Jain A., "Speckle reduction using multiple tones of illumination," Appl. Opt. **12**, 1202–1212 (1973).

6. Furukawa A., Ohse N., Sato Y., Imanishi D., Wakabayashi K., Ito S., K.Tamamura, Hirata S., "Effective speckle reduction in laser projection displays," Proc. SPIE **6911**, 69110T (2008).

7. Zhang Y., Dong H., Wang R., Duan J., Shi A., Fang Q., Liu Y. "Demonstration of a home projector based on RGB semiconductor lasers," Appl. Opt. **51**, 3584 – 3589, (2012).

8. Redding B, Choma M. A., Cao H. "Speckle-free laser imaging using random laser illumination," Nature Photonics Letters **6**, 355–359 (2012).

9. Sarmani AR, Abu Bakar MH, Bakar AA, Adikan FR, and Mahdi MA., "Spectral variations of the output spectrum in a random distributed feedback Raman fiber laser," Opt. Expr. **19**(15), 14152-14159 (2011).

10. Rawson E.G., Nafarrate A.B., Norton R.E., and Goodman J. W., "Speckle-free rear-projection screen using two close screens in slow relative motion," J. Opt. Soc. Am. **66,** 1290–1294 (1976).

11. Kuratomi Y., Sekiya K., Satoh H., Tomiyama T., Kawakami T., Katagiri B., Suzuki Y., and Uchid T., "Speckle reduction mechanism in laser rear projection displays using a small moving diffuser" JOSA A **27** (11), 1812-1817 (2010).

12. Wang L., Tschudi T., Halldorsson T., and Petursson, "Speckle reduction in laser projection systems by diffractive optical elements," Appl. Opt. **37**, 1770-1775 (1998).

13. Kubota Sh., Goodman J.W. "Very efficient speckle contrast reduction realized by moving diffuser device," Appl. Opt. **49** (23), 4385-4391 (2010).

14. Trisnadi J.I., "Hadamard speckle contrast reduction," Opt. Lett. **29**, 11-13 (2004).

15. Trisnadi J.I. "Method, apparatus and diffuser for reducing laser speckle," U.S. patent 6,747,781 (8 June 2004).

16. Gao W. Tong, Zh., Kartashov V., Akram M.N., Chen X., "Replacing Two-Dimensional Binary Phase Matrix by a Pair of One-Dimensional Dynamic Phase Matrices for Laser Speckle Reduction," J. of Display Technology. **8** (5), 291-295 (2012).

17. Yang H.S., Yun S.K., Song J.H., An S.D., Park H.W., Shyshkin I., Yurlov V., and Lapchuk A., "SOM-based projection module for mobile displays" J. of the Society for Information Display **18 (**6)**,** 445–453 (2010).

18. Yun S.K., Song J., Lee T.W., Yurlov V., Park H.W., Park C., Kim H., Yang J., Cheong J., and Lapchuk A., "Spatial Optical Modulator (SOM): Samsung's Light Modulator for the Next Generation Laser Display,"IMID/IDMC '06 DIGEST (Proc. of Society for Information Display – SID. August), 29-1, 551-555 (2006).

19. Trisnadi J.I., Carlisle C.B. and Monteverde v, "Overview and applications of Grating Light ValveTM based optical write engines for high-speed digital imaging," MOEMS Display and

Imaging Systems II, edited by Hakan Urey, David L. Dickensheets, Proc. SPIE **5348**, 52-64 (2004).

20. Kowarz M.W., Brazas J.C., and Phalen J.G., "Conformal Grating Electromechanical system (GEMS) for High-Speed Digital Light Modulation," IEEE, 15th Int. MEMS Conf. Digest, 568-573 (2002).

21. Sprague R., Champion M., Brown M., Brown D., Freeman M., and Niesten M., "Mobile Projectors Using Scanned beam Displays", from Mobile Displays, Technology and Applications, Bhowmik, Li, and Bos editors, John Wiley and Sons, Chapter 21, 2008.

22. Davis W.O., Sprague R., and Miller J., "MEMS-Based Pico Projector Display", Proc. IEEE/LEOS Opt. MEMS & Nanophoton. pp. 31-31(2008).

23. Yurlov V., Lapchuk A., Yun S., Song J. Yeo I, Yang H, and An S., "Speckle suppression in scanning laser displays: aberration and defocusing of the projection system," Appl. Opt. **48**, 80-90 (2009).

24. Akram M.N., Kartashov K., and Tong Zh., "Speckle reduction in line-scan laser projectors using binary phase codes," Opt. Lett. **35**, 444-446 (2010).

25. Tong. Zh., Chen X., Akram M.N., and Aksnes A., "Compound Speckle Characterization Method and Reduction by Optical Design"// J. of Display Technology. **8**, N3, 132-137 (2012).

26. An S.-D., Lapchuk A., Yurlov V., Song J.H., Park H.W., Jang J.W., Shin W.C., Kargapoltsev S., Yun S.-K. Speckle suppression in laser display using several partially coherent beams 5 January 2009 / Vol. 17, No. 1 / Opt. Expr. 92, p. 92-103.

27. Kohler D., Seitz W.L., Loree T.R., and Gardner S.D., "Speckle reduction in pulsed-laser photographs," Opt. Commun. **12**(1), 24–28 (1974).

28. M. J. Sun and Z. K. Lu, "Speckle suppression with a rotating light pipe," Opt. Eng. V. 49, N2, pp. 024202-024202-6 (2010).

29. Mehta D.S., Naik D.N., Singh R.K., and Takeda M., "Laser speckle reduction by multimode optical fiber bundle with combined temporal, spatial, and angular diversity," Appl. Opt. **51**(12), 1894-1904 (2012).

30. B. Dingel, S. Kawata, and S. Minami, "Speckle reduction with virtual incoherent laser illumination using a modified fiber array," Optik (Stuttg.) **94**, 132–136 (1993).

31. 4. B. Dingel and S. Kawata, "Speckle-free image in a laser-diode microscope by using the optical feedback effect," Opt. Lett. **18**(7), 549–551 (1993).

32. 5. J. Kim, E. Kim, D. T. Miller, and T. E. Milner, "Speckle reduction in OCT with multimode source fiber," Proc. SPIE **5317**, 246–250 (2004).

33. J. G. Manni1, J. W. Goodman "Versatile method for achieving 1% speckle contrast in large-venue laser projection displays using a stationary multimode optical fiber" Opt. Expr. **20** (10), 11288- 11312 (2012).

34. Goodman J. W. "Statistical Optics" Wiley, 2000.

35. P. Borwein P., Mossinghoff, M. J. "Barker sequences and flat polynomials". Number Theory and Polynomials. LMS Lecture Notes. **352**. Cambridge University Press. (2008). pp. 71–88.

36. M. Born, E. Wolf, *Principles of Optics* (Cambridge University Press, 1999).

Figure captions

- Fig.1. Optical scheme of the laser projector with two Barker code-type DOEs.
- Fig. 2. Cross-section of the Barkercode-type DOE and the corresponding Barker code sequences.
- Fig. 3. Barker code-type DOE of length 7 - (a) and the autocorrelation function $A(x)$ - (b) and $A_0(x)$ - (c) for different values of N (not scaled).
- Fig. 4. Q(x).
- Fig. 5. Dependence of the speckle contrast (simulation results) on the ratio of the eye's (photo camera) lateral resolution (on the distance of the eye to the screen – upper axis) to the DOE period calculated with different formulae: solid line – exact formula. a) $N = 7$ and b) $N = 13$; S_0 is the distance where $D_0 = NT$.
- Fig. 6. Dependence of the speckle suppression coefficient k_{sp}^{y} and the optical efficiency on the wavelength for different numerical apertures, NA_1, of the objective lens of the projector.
- Fig.7. Dependence of the autocorrelation function $A(y)$ of the screen (along the y direction) on the wavelength (simulation results): $NA/(l/T) = 5$; $N = 13$.
- Fig.8. Dependence of the speckle suppression coefficient k_{sp}^{y} on NA ($N = 13$) for blue, red and green laser beams.
- Fig. 9. Dependence of the optical efficiency of the speckle suppression method on the NA (N=13).
- Fig. 10. Dependence of the autocorrelation function $A(y)$ on the NA: $\lambda = 0.53\,\mu m$; $N = 13$.

- Fig. 11. Dependence of the speckle suppression coefficient k_{sp}^{x} on the numerical aperture of the objective lens for laser beam of different colors.
- Fig. 12. Dependence of A_0 on NA for $l = l_{gr} = 0.53$ μm.
- Fig. 13. $A_0(x)$ for different NA: $l_{bl} = 0.40$ mm; $N = 13$.

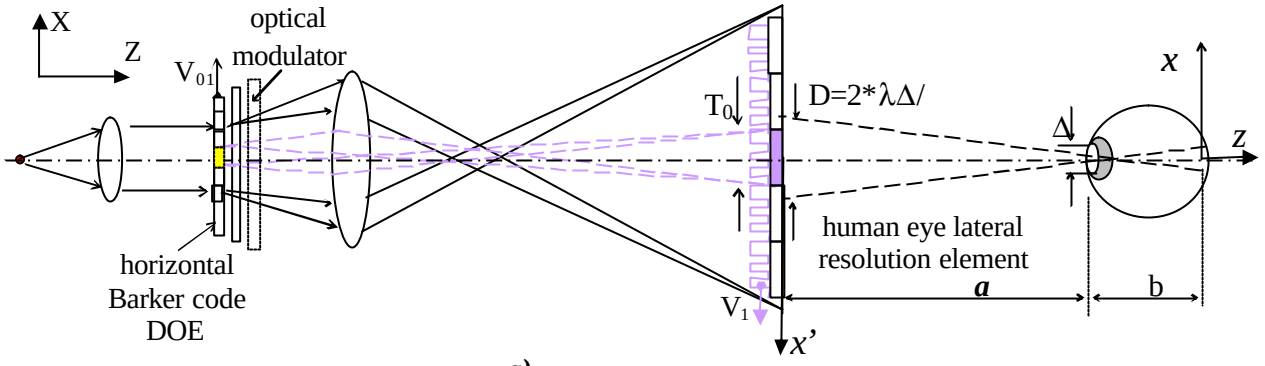
X
Z
optical
modulator
V01
T0
D=2*λΔ/
x
Δ
z
human eye lateral
resolution element
a
b
horizontal
Barker code
DOE
V1
x'

a)

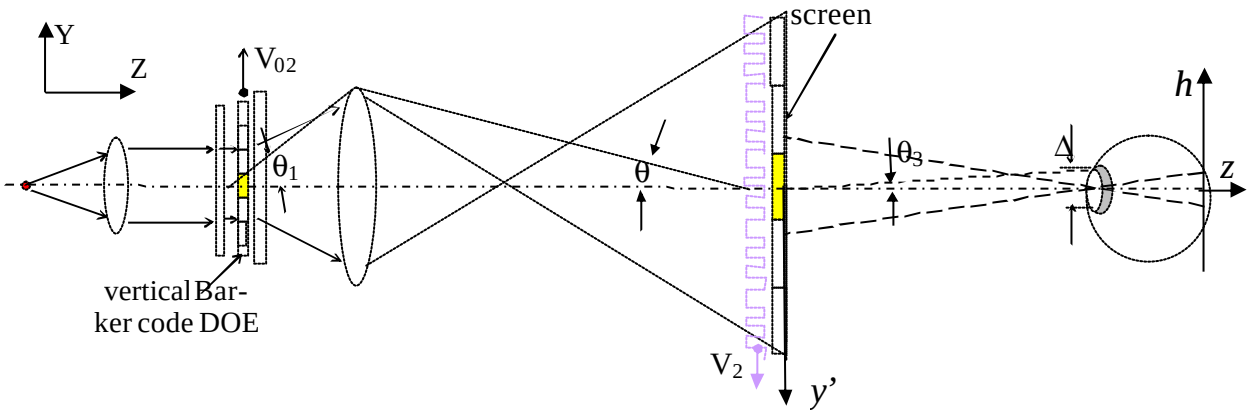
Y
Z
V02
screen
h
θ1
θ
θ3
Δ
z
vertical Bar-
ker code DOE
V2
y'

b)

Fig.1.

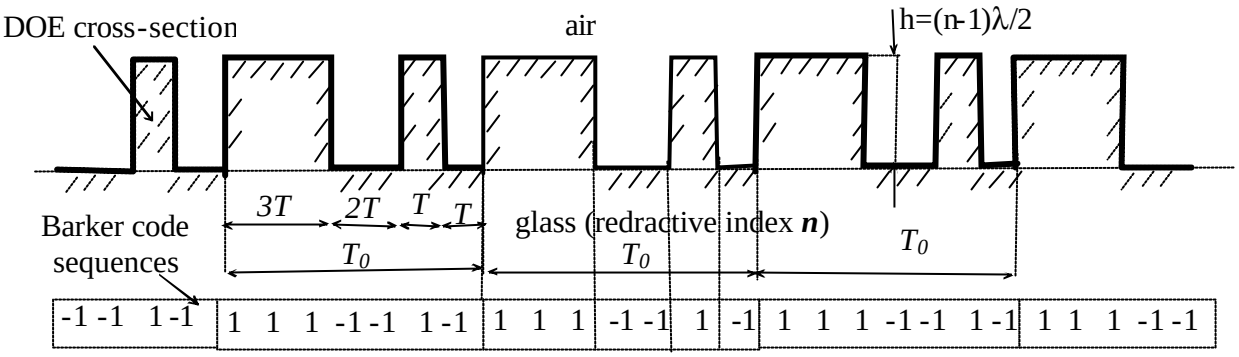
DOE cross-section
air
h=(n-1)λ/2
3T
2T
T
T
Barker code sequences
glass (redractive index n)
T0
T0
T0
-1 -1 1 -1
1 1 1 -1 -1 1 -1
1 1 1
-1 -1
1
-1
1 1 1 -1 -1 1 -1
1 1 1 -1 -1

Fig. 2.

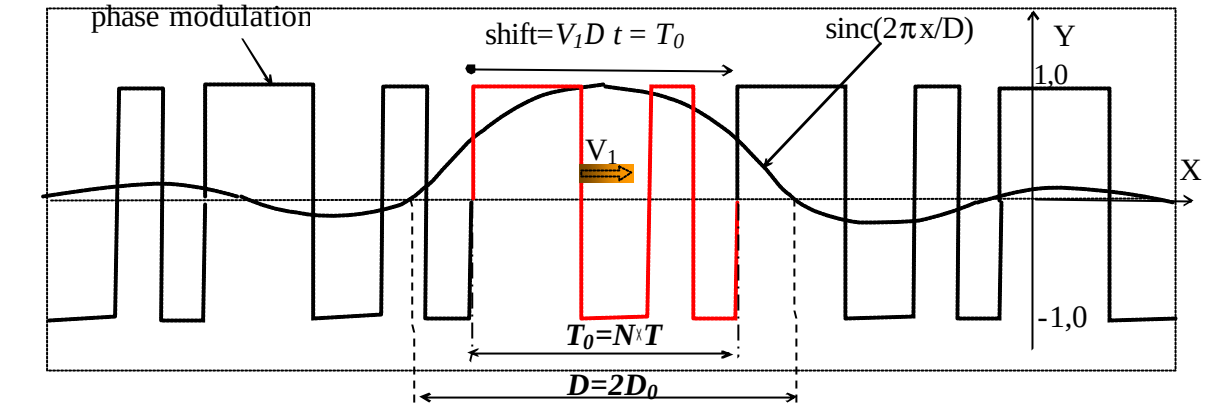
phase modulation
shift=V_1D $t = T_0$
sinc(2πx/D)
Y
1,0
X
V_1
-1,0
$T_0=N^xT$
$D=2D_0$

(a)

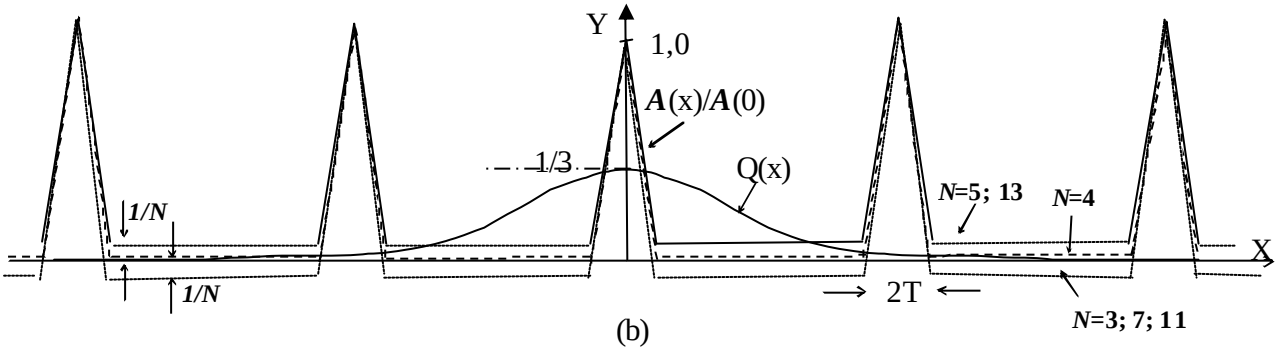
Y
1,0
$A(x)/A(0)$
1/3
Q(x)
N=5; 13
N=4
X
1/N
1/N
2T
N=3; 7; 11

(b)

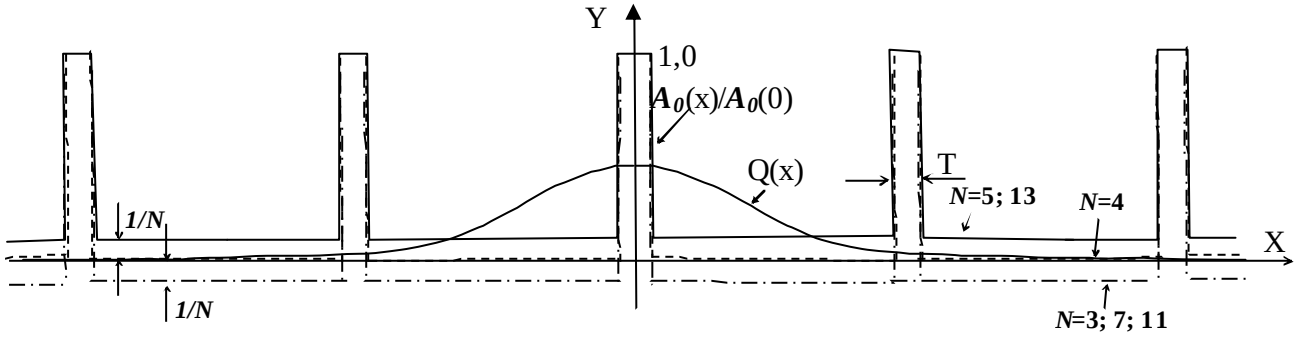
Y
1,0
$A_0(x)/A_0(0)$
Q(x)
T
N=5; 13
N=4
X
1/N
1/N
N=3; 7; 11

(c)

Fig. 3.

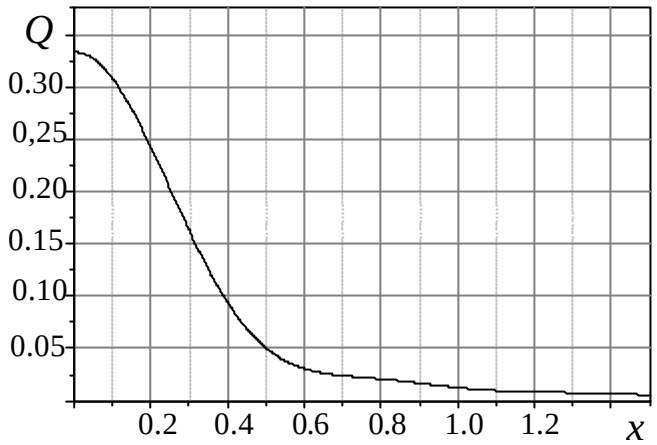

Fig. 4.

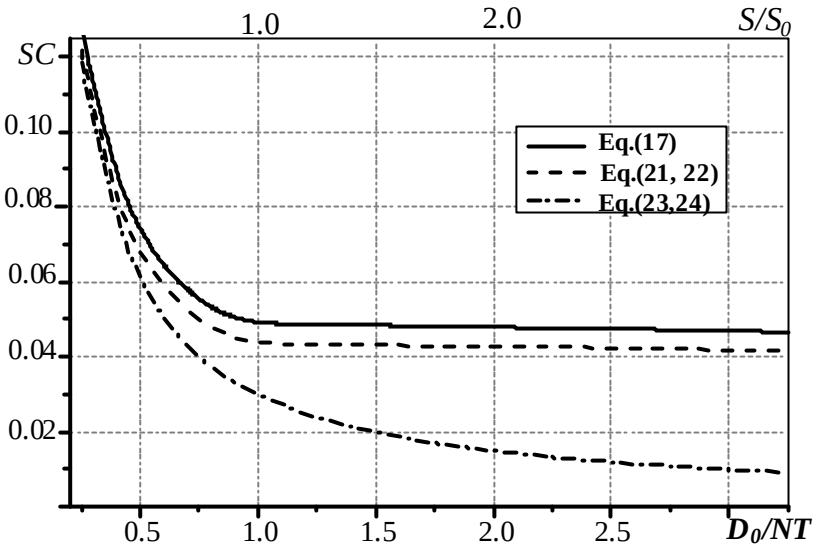
1.0
2.0
S/S0
SC
0.10
0.08
0.06
0.04
0.02
Eq.(17)
Eq.(21, 22)
Eq.(23,24)
0.5
1.0
1.5
2.0
2.5
D0/NT

(a)

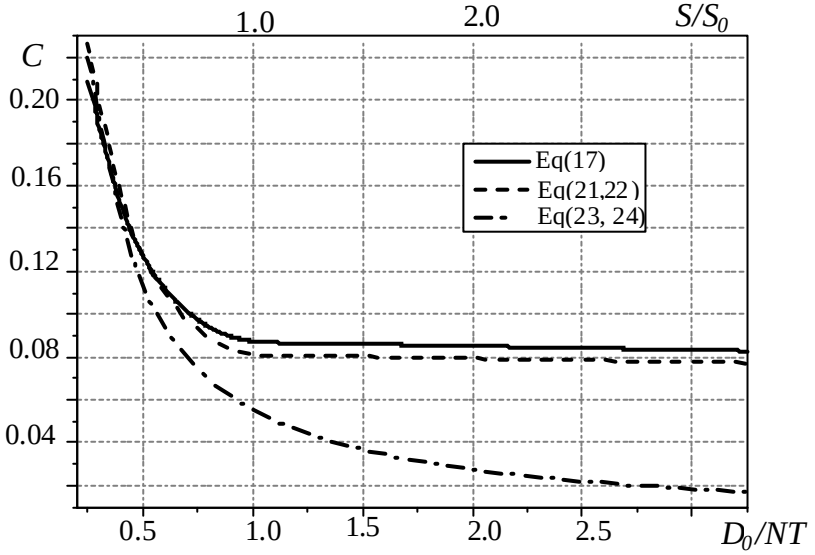
1.0
2.0
S/S0
C
0.20
0.16
0.12
0.08
0.04
Eq(17)
Eq(21,22)
Eq(23, 24)
0.5
1.0
1.5
2.0
2.5
D0/NT

(b)

Fig. 5.

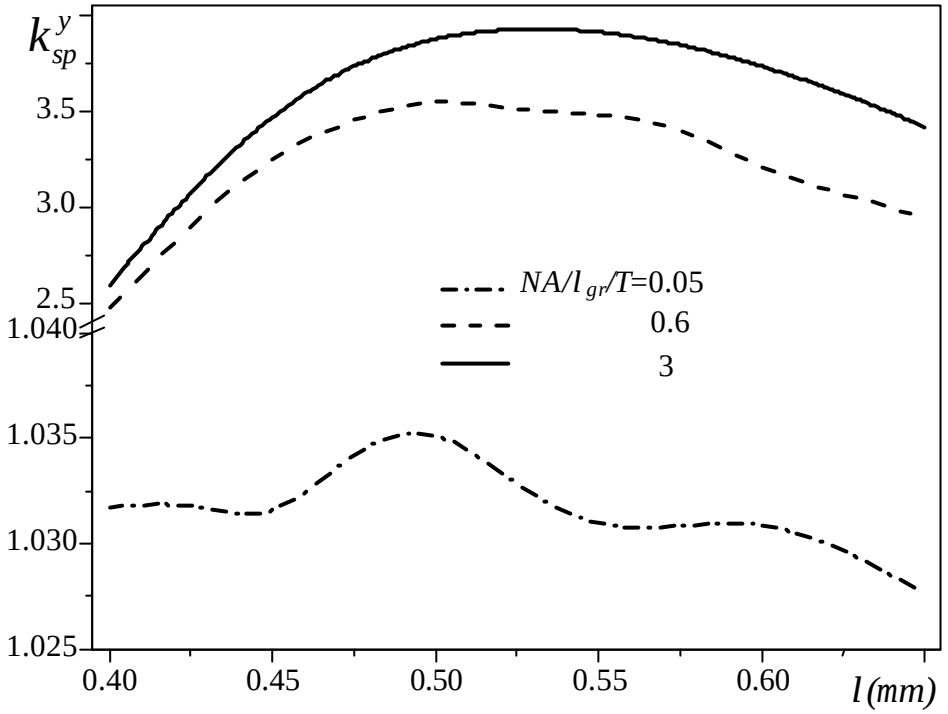
k_{sp}^{y}
3.5
3.0
2.5
1.040
1.035
1.030
1.025
0.40
0.45
0.50
0.55
0.60
$l\,(mm)$
$NA/l_{gr}/T$=0.05
0.6
3

Fig. 6.

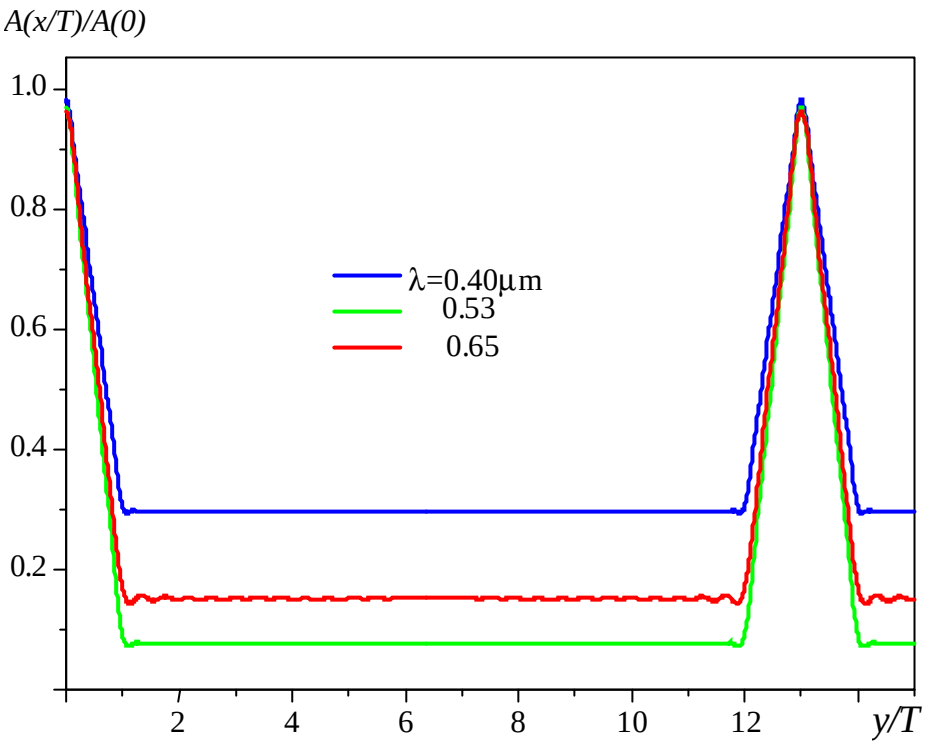

Fig.7.

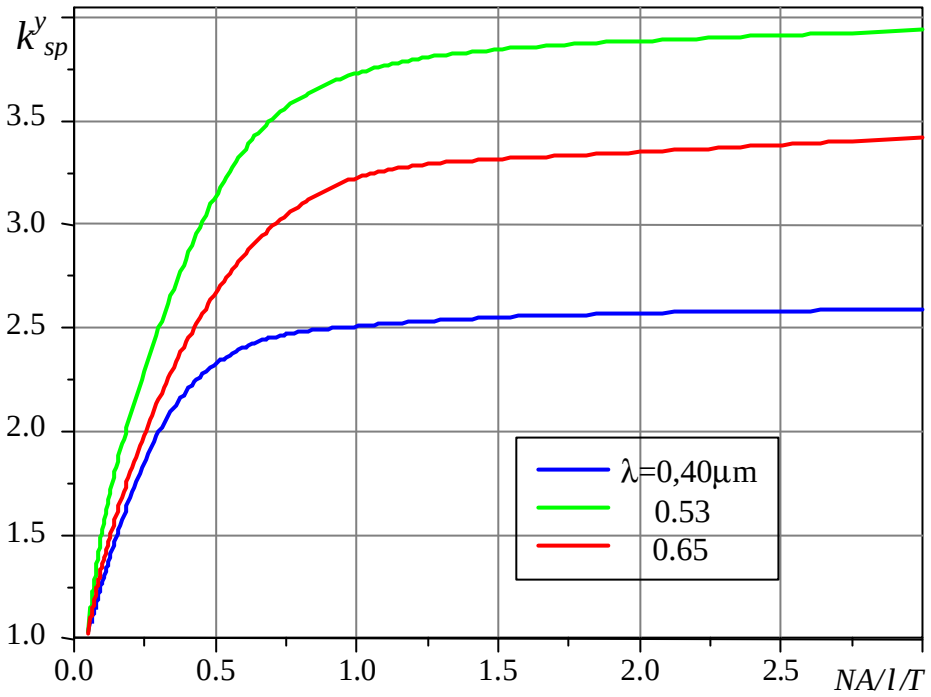

Fig.8.

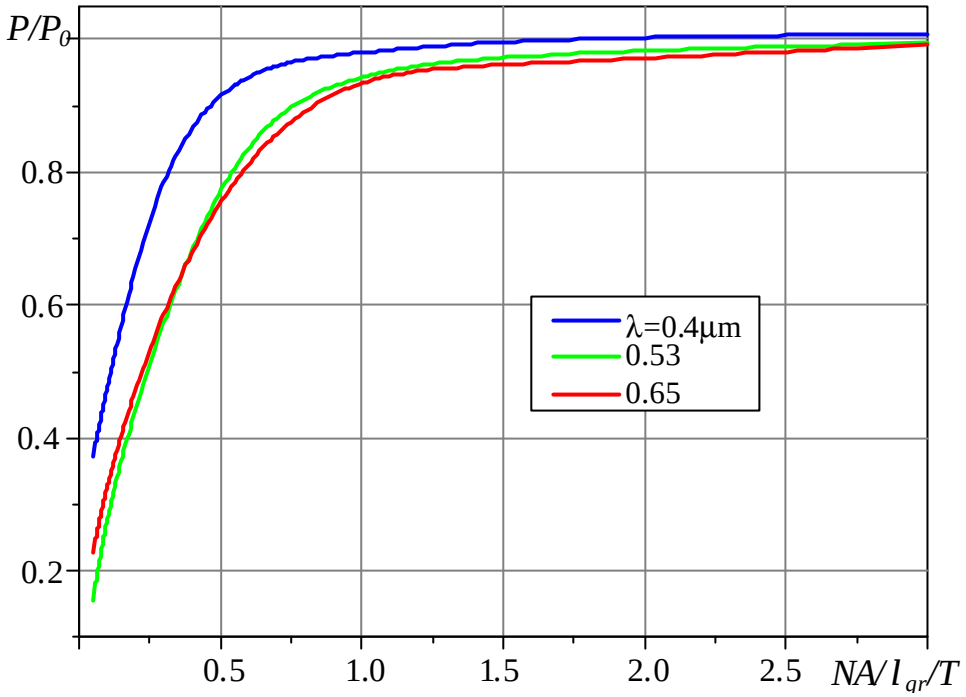

Fig. 9.

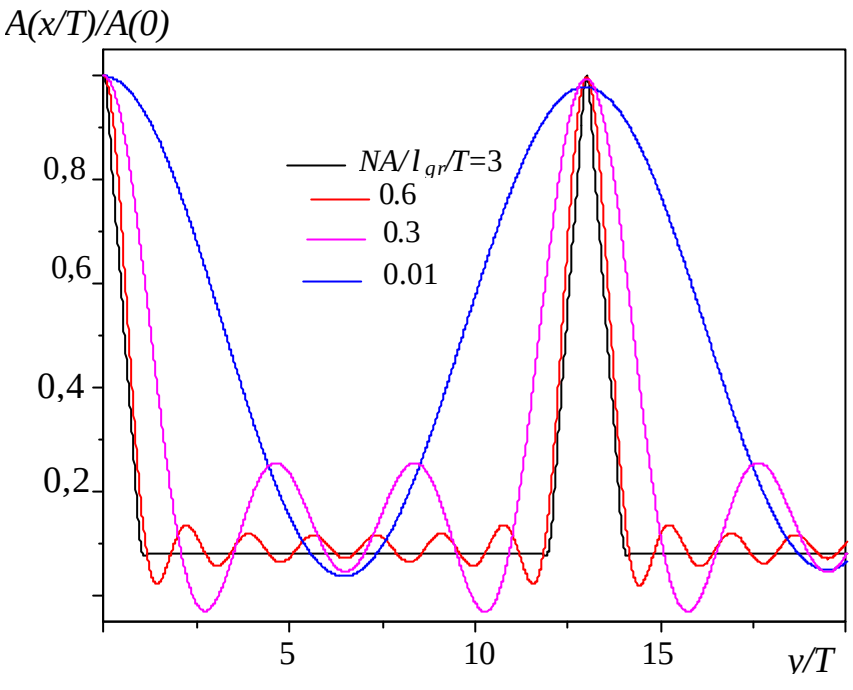

Fig. 10.

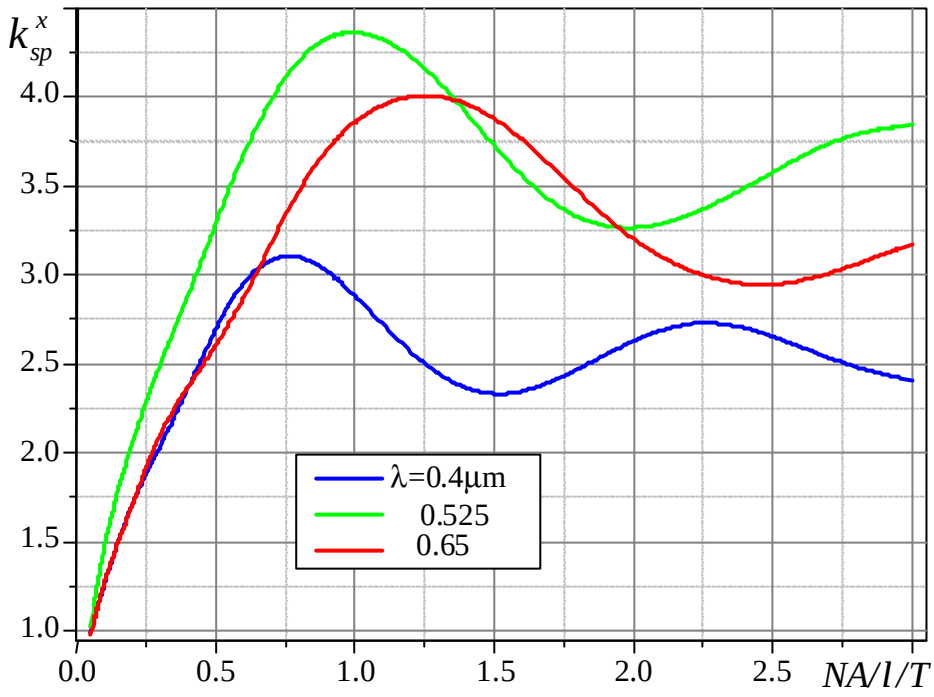

Fig. 11.

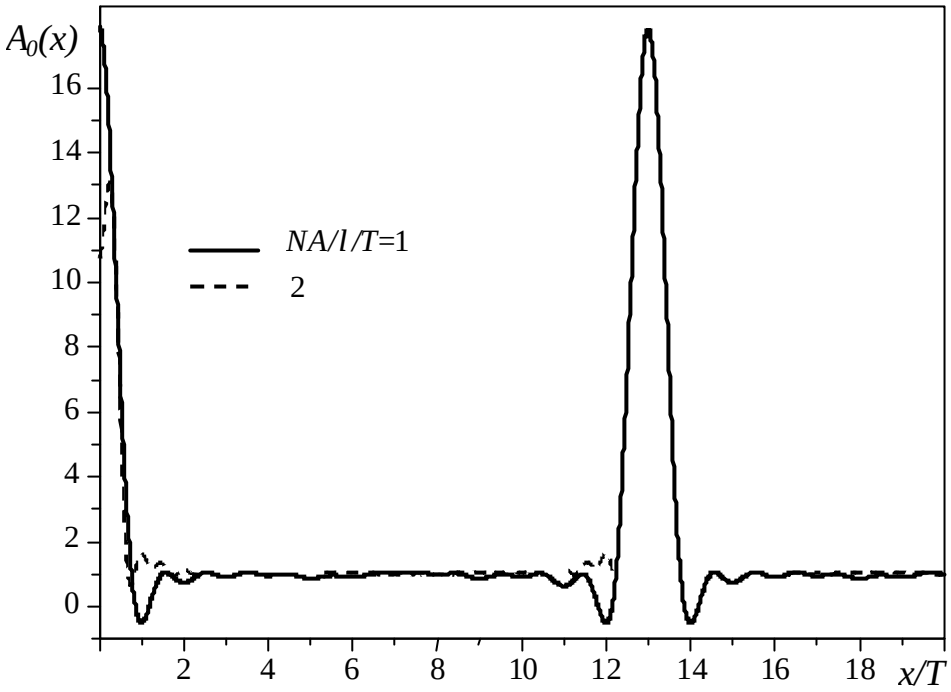

Fig. 12.

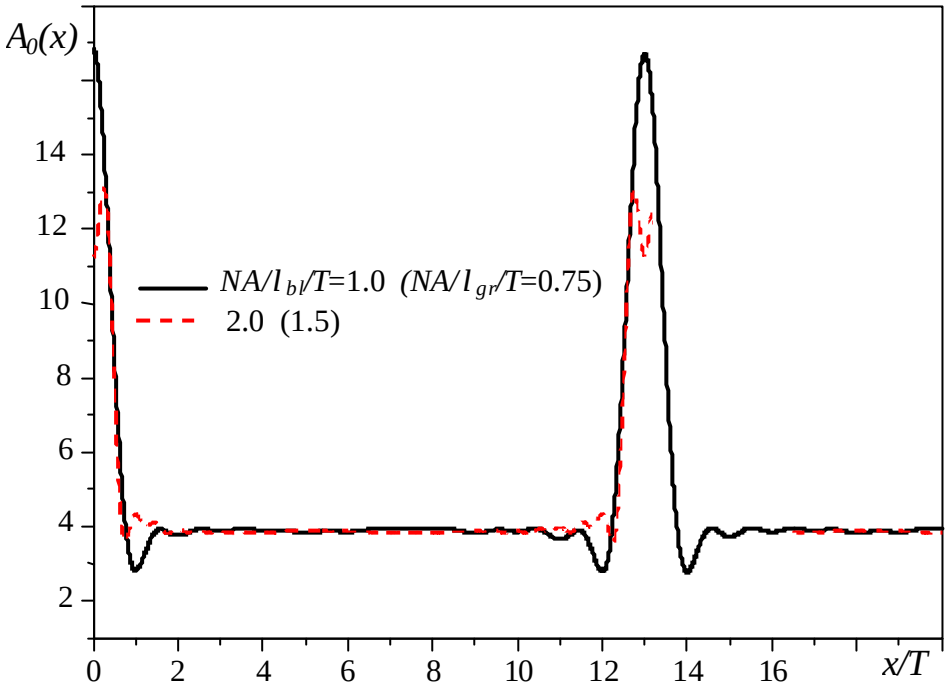

Fig. 13.